Radiopaque, Barium Sulfate-Filled Biomedical Compounds of a Poly(Ether-Block-Amide) Copolymer

Xiaoping Guo

St. Jude Medical, Inc., 14901 DeVeau Place, Minnetonka, Minnesota 55345

ABSTRACT: Various radiopaque compounds of a poly (ether-*block*-amide) copolymer resin filled with fine barium sulfate particles were prepared by melt mixing. Material properties of the filled compounds were investigated using various material characterization techniques, including thermogravimetric analysis (TGA), differential scanning calorimetry (DSC), dynamic rheometry, uniaxial tensile test, and dynamic mechanical thermal analysis (DMTA). The effects of the filler and its concentration on the measured material properties are evaluated. It has been found that in addition to its well-known X-ray radiopacity, the filler is quite effective in reinforcing some mechanical properties of the copolymer, including modulus of elasticity and yield strength. More interestingly, it has been observed that at low loading concentrations near 10 wt %, the filler may also act as a rigid, inorganic toughener for the copolymer by improving the postyield material extensibility of strain hardening against ultimate material fracture. © 2008 Wiley Periodicals, Inc. J Appl Polym Sci 109: 4015–4024, 2008

Key words: poly(ether-*block*-amide); polyamide-based thermoplastic elastomer; barium sulfate; DSC; TGA; DMTA; dynamic rheometry

INTRODUCTION

Because of increasing rigorous needs in medical device industry, specialty biomedical polymer compounds, instead of pure industrial polymer resins, are required in the manufacturing of cardiac and endovascular devices that are designed to insert into the human body for critical diagnostic and/or surgical medical procedures. Such a polymer compound commonly contains an essential additive, called radiopaque filler or radiopacifier, which renders the image visibility of a medical device inside the human body under an X-ray fluoroscope. The particles of the filler dispersed in the polymer matrix can significantly increase the overall density of the compound and thus attenuate X-ray radiation energy differently than soft tissues and bones. This would provide the contrast and sharpness of the X-ray fluorescent image for the device, so that a physician could accurately position and locate the device in the body during the medical procedure. The types and amounts of the radiopaque fillers used for the specialty medical compound of a polymer will not only affect the quality of the X-ray image of the device, but also, more or less, change the mechanical, rheological, and thermal properties of the host polymer. The latter would inevitably affect the functionality and end-use performance of the medical device. Up to date, most radiopaque fillers used in medical device industry are originally derived from heavy metals, such as tungsten, gold, and platinum, or inorganic mineral substances containing certain heavy metals, such as barium sulfate, bismuth subcarbonate, bismuth trioxide, and bismuth oxychloride. The particles of selected radiopaque filler are generally incorporated into a polymer matrix via conventional melt mixing or compounding technology. Because of its high thermal stability, excellent biostability and biocompatibility, chemical inertness, and low cost as well as a variety of coloring options for the resultant medical compounds, barium sulfate ($BaSO_4$), especially in the spherical powder form of ca. 0.5–2.0 μm in diameter, is most commonly chosen for preparing radiopaque polymer compounds that are used in various disposable medical devices, such as cardiac introducers, angiographic catheters, electrophysiology diagnosis catheters, ablation catheters, and the like.

Barium sulfate is chemically purified from a common mineral substance, called barite, barytes, or heavy spar. It can occur in a variety of natural rocks, including limestone and sandstone. Chemically, $BaSO_4$ can be considered as an inorganic salt with a lattice of ions, Ba^{2+} and SO_4^{2-}. It has been reported

that $BaSO_4$ is monopolar in nature, exhibiting electron-donor ability with essentially zero value for its electron-acceptor component in the surface free energy.[1] Thus, for a nonpolar polymer (i.e., polyethylene and polypropylene), a coupling agent may be necessary for encapsulating $BaSO_4$ particles to form so-called core-shell structure.[2–5] However, for a polar polymer, there may exist inherent special interactions between the polymer and the filler surfaces, such as ionic pairs, hydrogen bonding, and van deWaal forces. Hence, $BaSO_4$ particles may be conveniently dispersed and incorporated into the polar polymer matrix via high shear mixing without using any coupling agent. In this study, we were in an attempt to study a typical polar polymer compound filled with $BaSO_4$. Because of its wide applications in medical devices industry, a poly(ether-*block*-amide) copolymer (PEBA) resin, commonly known as a polyamide-based thermoplastic elastomer, was selected as host polymer.[6,7] It is a typical-segmented block copolymer with $(A − B)_n$ backbone structure, in which the hard blocks consist of crystallizable polyamide 12 (PA) segments, and the soft blocks are composed of poly(tetramethylene oxide) (PTMO) segments with subambient glass transition at about −75°C.[6,8] The two blocks are chemically connected via an ester linkage. Its chemical structure can be illustrated as the following scheme:

$$HO \left[\overset{\overset{O}{\parallel}}{C} - PA - \overset{\overset{O}{\parallel}}{C} - O - PTMO - O \right]_n H \quad (1)$$
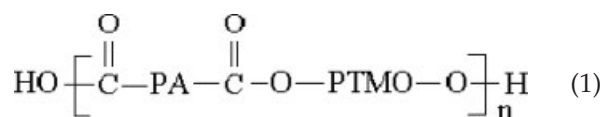
It has been reported in literature[6,9–14] that the PA segments generally crystallize in lamellar structures, which can further self-organize into larger spherulitic superstructures if the PA/PE molar mass ratio is greater than one. These crystalline PA phases or microdomains form a physical crosslink network in the copolymer and affect some mechanical properties, such as elastic modulus and hardness. On the other hand, PE segments form amorphous phases or microdomains and act as entropic springs, primarily affecting the flexibility and resiliency of the PEBA copolymer.

In spite of widespread applications of radiopaque, $BaSO_4$-filled PEBA compounds, especially in various disposal medical devices, there is few research work reported in literature so far. Therefore, in this study, we have dealt with investigating the effects of $BaSO_4$ radiopaque filler and its loading concentration on various common material properties of a PEBA copolymer. This would enlighten our understanding on the filled PEBA compounds with different compositions in an aim to obtain synergistic balance among various material property attributes for the

sake of optimum end-use material performance in the medical devices.

MATERIAL CHARCATERIZATION TECHNIQUE

Materials of study

The PEBA copolymer resin used in this study was acquired from a well-established commercial source, Pebax® 7233 SA01 MED (Arkema, Inc.). It is an additive-free biomedical grade resin, having the melt-flow-index of 5.5 g/10 min measured at 235°C 1 kg per ASTM D1238. The radiopaque filler used is a high-purity pharmaceutical grade, Barium Sulfate 4518, purchased from Mallinckrodt. Per specification from the vendor, the nominal diameter of the spherical filler particles is ~ 0.65 μm with the diametrical size distribution from 0.1 μm to a value less than 1.0 μm. To avoid the possibility of moisture-induced hydrolysis of the PEBA copolymer during melt compounding, the resin and filler as received were dried at 75 and 120°C for 12 h in vacuum oven, respectively. A laboratory-scale compounding system, Eurolab™ 16 mm, 40 : 1 L/D modular twin-screw extruder (Thermo Fisher Scientific), was used to prepare various radiopaque PEBA compounds. Prior to uses in various material characterization experiments to be discussed below, the pelletized PEBA compounds were dried at 75°C for 8 h in a vacuum oven.

General thermal analysis

To understand the effect of $BaSO_4$ and its loading concentration on the general melting and crystallization behaviors for various radiopaque PEBA compounds, TGA and DSC experiments were conducted under nitrogen atmosphere in a Q5000IR TGA instrument (TA Instruments, Waters LLC) and Pyris-1 DSC instrument equipped with an intracooler (PerkinElmer), respectively. For TGA measurements, temperature reading was first calibrated based on the Curie points measured at a scanning rate of 20°C/min with dry nitrogen purge gas flowing at 20 mL/min. Three calibration substances, including alumel, nickel, and 83 : 17 nickel-cobalt alloy, were used. Thermal stability of the filled PEBA compounds was measured by heating the pellet-shaped samples weighing about 25 mg from 50 to 800°C at the same scanning rate of 20°C/min. For DSC study, the heat-flow and temperature readings of the instrument were calibrated with a high purity indium standard at the scanning rate of 10°C/min. The compound samples were prepared by cutting the compound pellets into the form of thin films with a sharp blade. A relatively small mass of the sample, weighing ~ 4.0 mg, was taken and hermetically sealed in the DSC pan to minimize the effects

of thermal lag in the DSC cell during the scans. Thermal program used for the DSC calorimetric experiments primarily consisted of two heating scans from 0 to 220°C at the scanning rate 10°C/min, between which there was a cooling scan at 20°C/min. The DSC thermographs obtained in the cooling and second heating scans were analyzed for the interpretation of crystallization and melting behaviors of the PEBA compounds, respectively.

Dynamic rheometry

The influences of $BaSO_4$ filler on rheological behaviors of the filled PEBA compounds were studied via a controlled-strain rotational rheometer, ARES-RDA III (TA Instruments, Waters LLC) equipped with a convection oven. To prevent possible thermal degradation of the samples in the oven at melt temperature, pressurized N_2 gas flowing at 60 Psig was used as the convective medium. Parallel-plate configuration with the plate diameter of 25 mm was used. The two plates were set at a constant gap of 1.5 mm for all dynamic rheological tests. These tests, namely the frequency sweeps from 0.25 to 500 rad/s, on pure resin and its filled compounds were conducted under given strain amplitude of 15% and melt temperature of 200°C. Storage modulus (G') and loss modulus (G'') were measured at eight data points per decade of frequency (ω). Accordingly, the real and imaginary parts of complex viscosity (η^*), η', and η'' are calculated, respectively, as the following:

$$\eta' = \frac{G''}{\omega} \tag{2}$$

$$\eta'' = \frac{G'}{\omega} \tag{3}$$

$$\eta^* = \eta' + i\eta'' \tag{4}$$

It is worthwhile to note that for a typical block copolymer, there exists microphase separation temperature (MST) or order–disorder temperature (ODT), at its molten states.[15–17] Considering the fact that the MST for the copolymer (namely, Pebax 7233 resin)[18,19] is ca. 180°C, the dynamic rheometry was selectively conducted at melt temperature of 200°C, at which the molten states of the copolymer resin and filled compounds would be surely isotropic and lack of any microphase-separated structure. In addition, the frequency range used for the study was limited by the instrument torque transducer and determined to be within the sweep from 0.25 to 500 rad/s. This is to ensure that complex viscosity and other dynamic properties were derived from the reliable values of measured torques by the instrument. Importantly, with linear viscoelasticity of measurement taken into account for the whole frequency range of concern, constant strain amplitude, i.e., 15%, was chosen for all dynamic rheometry experiments at 200°C.

Uniaxial tensile test

Type 1BA dumbbell-like tensile bars per the geometry specified in ASTM D5937 (or ISO 527-2) were molded for pure resin and the filled compounds using a Minijet™ micromolding press (Thermo Fisher Scientific) and a house-made mold under mold and melt temperatures at 50 and 220°C, respectively. Uniaxial tensile curves of engineering stress (σ) versus Cauchy strain (ε) were measured at the crosshead speed of 500 mm/min and the gauge length of 30 mm (or the strain rate at 27.78% s) using a tensile tester, Model 5564 test frame (Instron) equipped with ReNew™ control electronics and Testwork™ software (MTS Systems). At least five specimens were measured for each filled PEBA compound to obtain its averaged mechanical properties.

Dynamic mechanical thermal analysis

Rectangular DMTA bars having the geometry of 50.0 × 9.8 × 0.9 mm were prepared with a house-made mold using the Minijet press under the same condition as stated in Uniaxial tensile test section. Dynamic mechanical thermal properties of the filled PEBA compounds in their solid states were measured using a strain-controlled instrument, RSA III (TA Instruments, Waters LLC), equipped with a convection oven and a liquid-nitrogen (LN_2) cooling accessory. Also, the evaporated LN_2 flowing into the oven serve as the convective medium to avoid possible oxidation of a test sample during the long time DMTA test, especially within high temperature region. The temperature step scans were conducted under isochronal conditions over the wide temperature range from −120 to 170°C at angular frequency of 5 rad/s. Sample soak time at each temperature step is 1 min to truly attain isothermal states for the measurement. The small strain amplitudes, which were automatically adjustable from 0.005 to 0.100% as the temperatures were increased, were maintained by means of the static autotension and dynamic autostrain control of the instrument. This would assure that the DMTA measurement was well within the viscoelastic region over the whole temperature range.

RESULTS AND DISCUSSION

Thermal stability

The TGA thermographs for various $BaSO_4$-filled PEBA compounds are shown in Figure 1. It can be
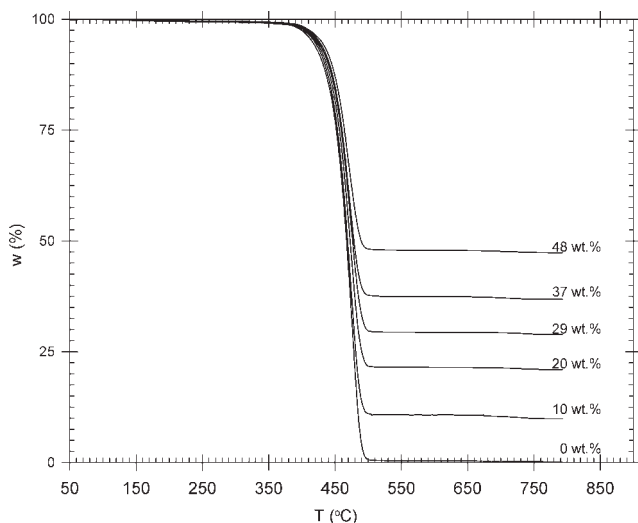
Figure 1 TGA thermographs for various filled PEBA compounds at different loading concentrations of BaSO$_4$.

observed that pure resin was thermally degraded to almost zero weight. This fact allows one for determining actual BaSO$_4$ loadings in the compounds as obtained by melt compounding, and the results are indicated in the figure. Also, it can be realized from the TGA thermographs that the BaSO$_4$ filler is chemically inert to the PEBA copolymer, exhibiting high thermal stability at temperatures as high as 800°C. The filler might marginally improve, or at least, has no detrimental effects on the thermal stability of the PEBA copolymer when incorporated into the compound.

Characteristics of melting and crystallization

In an attempt to study the effects of BaSO$_4$ filler on general melting and crystallization characteristics of the PEBA copolymer, Figure 2 is plotted to show the DSC thermographs for pure PEBA resin and a representative filled compound containing 29 wt % BaSO$_4$ in terms of the normalized heat flow per unit mass (ΔQ^*) versus temperature (T). In the figure, the exotherms, namely curves 1 and 2, are attributed to the calorimetric events of nonisothermal crystallization for the filled compound and neat PEBA resin, respectively. These exotherms were measured at a rate of 20°C/min of cooling from the isotropic melt at 220 to 0°C. Then, the endotherms, as denoted by curves 3 and 4 for the filled compound and pure resin, respectively, were recorded at a rate of 10°C/min upon the subsequent step of heating the so-crystallized samples from 0 to 220°C. These endotherms are primarily associated with the melting of crystalline PA microdomain of the PEBA copolymer.

From Figure 2, one can realize by comparing curve 1 with 2 that melt crystallization of the copolymer

was drastically changed by the incorporation of BaSO$_4$ filler. The filled PEBA compound apparently starts to crystallize at higher temperature with its exotherm occurring within much narrower temperature region than pure resin. These facts suggest that BaSO$_4$ filler can appreciably increase crystallization temperature and distinctly accelerate the process of melt crystallization of the PEBA copolymer. Therefore, BaSO$_4$ filler can be considered as an effective, inorganic nucleating agent for the PEBA copolymer. With regard to general melting characteristics as revealed in curves 3 and 4 for the filled compound and pure resin, respectively, it is noticed that there seems to have some differences in their DSC heating thermographs. In details, when crystallized under the same "apparent" condition by cooling the melts from 220 to 0°C at a rate of 20°C/min, the filled compound exhibited dual endotherms, whereas pure resin showed a single endotherm along with a small, preceding exotherm, upon the subsequent DSC heating scan. However, their primary endotherms are located at the same peak temperature, ca. 171.0°C.

It has been reported by our previous study[20] that dependent of certain condition of melt crystallization, the crystallized PEBA copolymer may give rise to single or dual endotherms when subject to the subsequent DSC heating. Similar melting behaviors were also reported for thermoplastic polyurethane block copolymers.[21,22] In particular, for the PEBA copolymer, the effects of the early quenching step from the melt to crystallization temperature play a major role in determining the melting characteristics of the crystallized PEBA copolymer.[20] Such early quenching effects could be directly and qualitatively represented by the extent of supercooling, $\Delta T = T_m^0 - T_c$ where T_c and T_m^0 denotes crystallization tempera-
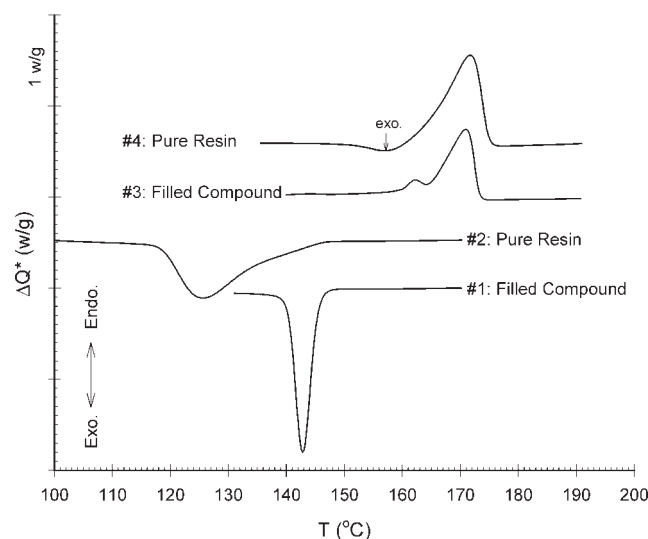

Figure 2 DSC thermographs for pure PEBA resin and a representative-filled PEBA compound.

tures and the equilibrium melting point for PA segments (which can be taken as 208.4°C[23]). In other words, the larger extent of supercooling ΔT, the larger effects of the early quenching would be on the melt crystallization and thus the melting characteristics of the so-crystallized copolymer. It is also noted from our previous study[20] that the crystallized PEBA copolymer with large quenching effect tends to exhibit a single-melting endotherm with the appearance of a small, preceding exotherm, whereas the one with minimal quenching effect is likely to display dual endotherms, when they are subject to the same DSC heating scan.

With the above discussion, one may be able to understand the effects of $BaSO_4$ filler on the melting behaviors of the PEBA copolymer. Because of the nucleating effects by the filler, the filled compound started to crystallize at higher temperature and at a faster rate than pure resin. Therefore, under the same ''apparent'' condition for melt crystallization, it is expected that the early quenching effect for the filled compound would be remarkably reduced. On the other hand, when compared with the filled compound, pure PEBA resin would experience the larger quenching effects due to lack of the filler-induced nucleating effect and slow crystallization rate. At the same time, this would lead to widening mixed PA/PTMO interphase with more amorphous PA segments trapped in the interphase due to such larger quenching effects. Therefore, during the subsequent DSC heating scan on the crystallized pure resin, a small exotherm preceding the primary endotherm (as noted in curve 4 of Fig. 2) could be attributed to the microphase demixing of some amorphous PA segments from the mixed PA/PE interphase when these PA segments are thermally reactivated.[20] Similar phenomena of microphase demixing have been observed calorimetrically for thermoplastic polyurethane block copolymers.[21,22]

Now, let us give some attentions on understanding the mechanisms for the dual endotherms shown in curve 3 of Figure 2 for the filled compound. First, it is noteworthy to point out that analogous to PA homopolymer,[23–25] the melt-crystallizable PEBA copolymer shows α- and γ-form polymorphism[6,14,20,26] and that the $\gamma \leftrightarrow \alpha$ crystal transformation, namely so-called Brill transition, could be reversible upon heating or cooling.[24] Calorimetrically, the PEBA copolymer may exhibit multiple melting endotherms. According to time-resolved X-ray diffraction investigation for PA homopolymer[24] and calorimetric study of various crystallized PEBA copolymers,[20] these dual endotherms as shown in curve 3 of Figure 2 could be attributed to the simultaneous events of (1) the melting of some low-temperature stable γ-crystals, which gives rise to the small endotherm, (2) the Brill transformation of the remaining γ-crystals into

the high-temperature stable α-crystals as temperature increases during the DSC heating scan, and (3) the melting of α-crystals, which results in the primary endotherm. In addition, the microphase demixing of the mixed interphases during the DSC heating scan promotes the Brill transition,[20] possibly leading to the complete $\gamma \rightarrow \alpha$-crystal transformation. As shown in curve 4 of Figure 2, this would result in the demixing exotherm, followed by a single endotherm for pure resin, which corresponds to the melting of high-temperature stable α-crystals only.

It is worthwhile to note that for various PEBA compounds filled with different loading concentrations of $BaSO_4$ from 10 to 47 wt %, there exist no significant differences in their melting and crystallization characteristics, including the onset and peak temperatures of melting and crystallization. The heats of fusion or crystallization per unit resin mass are about the same. In fact, as an effective nucleating agent, individual $BaSO_4$ particles serve as individual nucleus habits, from which crystals grow from the supercooled melt. On the other hand, because of the steric hindrance of $BaSO_4$ particles on polymer chain mobility, the increase in $BaSO_4$ loading concentration tends to slow down the arrangement of polymer molecules into ordered crystal lattices, although there may be more nucleus habits available for crystal growth. Therefore, there exists a critical loading level beyond which the nucleating effects of the filler become leveled off. Empirically, only a small amount, say 0.1–2%(v/v), is needed for an effective, inorganic nucleating agent. Any extra amount might not exhibit its influences on the host polymer in terms of crystallization and melting behaviors.

Rheological properties

The values of complex viscosity (η^*) as a function of frequency (ω) at 200°C for pure resin and its $BaSO_4$-filled compounds are shown in Figure 3. It can be observed that when compared with the viscosity value of pure resin, the viscosities for low $BaSO_4$-loading concentrations (say 10, 20, and 29 wt %) are slightly reduced within low frequency regions, but marginally increased within high frequency regions. With a further increase in the $BaSO_4$ concentration (i.e., 37 and 48 wt %), the viscosities of the compounds are considerably higher than that of pure resin within the whole frequency range used for the study. It is noted that a typical filled polymer melt may be of structured fluid exhibiting yielding behavior and its viscosity higher than that of host polymer under shear flow.[27–32]

To understand the above peculiar rheological observations, we need to explore the effects of the filler–filler interaction and polymer–filler interaction on dynamic viscosity. The former interaction
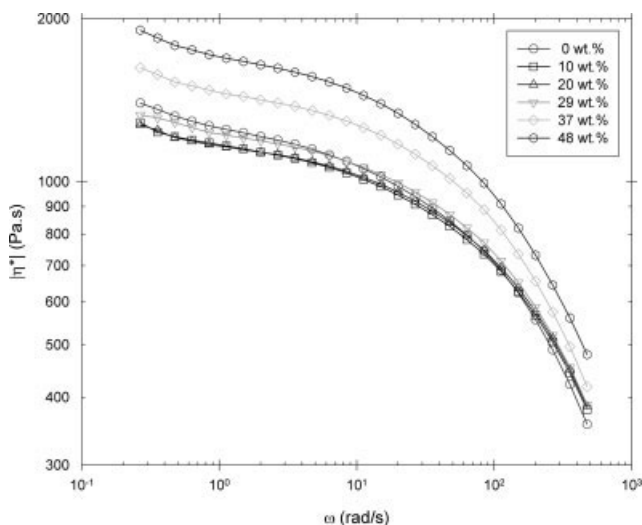
Figure 3 Complex viscosity values for various filled PEBA compounds at different loading concentrations of BaSO$_4$.

depends on statistical interparticle distance, although the latter is largely related to surface wetting of the filler particles by the copolymer. The combined effects of these interactions determine the extents of filler dispersion and agglomeration in the copolymer matrix, as shown in Figure 4, where various micrographs were taken on cross sections of the pellets taken from three representative filled compounds (i.e., 10, 29, and 48 wt %) using a scanning electron microscope (SEM), LEICA S430 (SEM-Leica Instrument). It can be observed from Figure 4(a) that at low BaSO$_4$ loading concentration (i.e., 10 wt %), a fine dispersion of BaSO$_4$ filler in the PEBA matrix was attained, possibly because of weak filler–filler interaction arising from large interparticle distances and strong polymer–filler interaction. The filler particles or microglobules are surrounded by fuzzy, diffuse polymer shells, possibly suggesting the polymer absorption onto the filler surfaces. Such adsorption may be favored by monopolar interactions between SO$_4^{2-}$ of the filler and (N···)H$^+$ of the PA segment of the copolymer, which would greatly promoted filler dispersion in the PEBA matrix. Furthermore, one may postulate that polymer adsorption by the filler results in the depletion of polymer-chain entanglements in the molten state.[30,32,33] Accordingly, per Doolittle free volume theory,[29,34] the compound melt may have its free volumes expanded, thus exhibiting the lower viscosity within low frequency regions at low BaSO$_4$-loading concentrations. The above viscosity reduction trend is gradually reverted as the frequency increases, and this indicates that the relaxation mechanism of the compounds must be different from that of pure resin due to the incorporation of the fillers. On the other hand, as the BaSO$_4$ concen-

tration increases, stronger filler–filler interactions develop due to closer interparticle distances. Hence, BaSO$_4$ particles are likely to form nonhydrodynamic, rigid particle aggregates. This trend of particle aggregation is clearly shown in Figure 4(b,c). Consequently, their presence in the melt may limit molecular mobility of thermally liable polymer chains and create steric hindrance. Hence, this would gradually degenerate the fluid state of the filled compounds and lead to a monotonic increase in the viscosity.[30–32] In addition, it can be also seen from Figure 3 that all the PEBA compounds exhibit shear thinning, and this behavior is commonly considered as being resulted from the non-Newtonian behavior of the molten polymer.
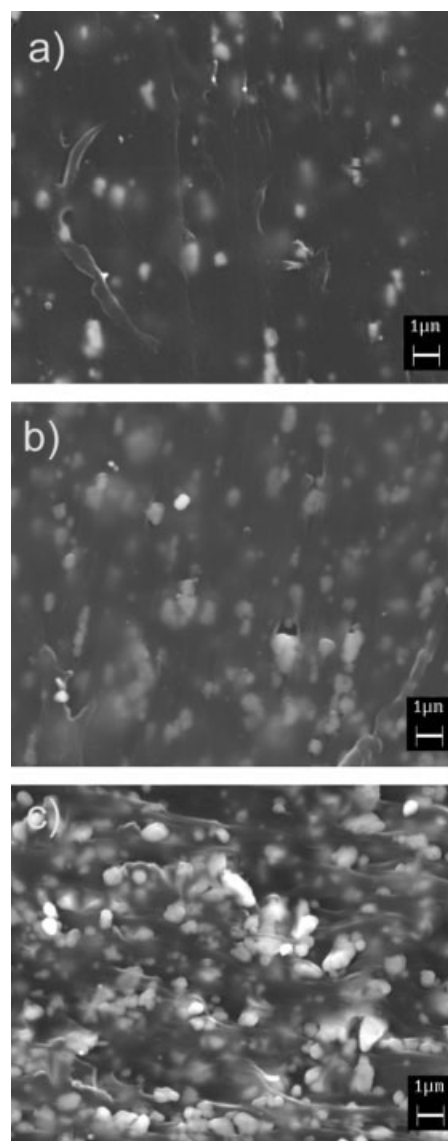

Figure 4 SEM micrographs taken on cross sections of pellets taken from filled PEBA compounds at three different loading concentrations of BaSO$_4$: (a) 10, (b) 29, and (c) 48 wt %.
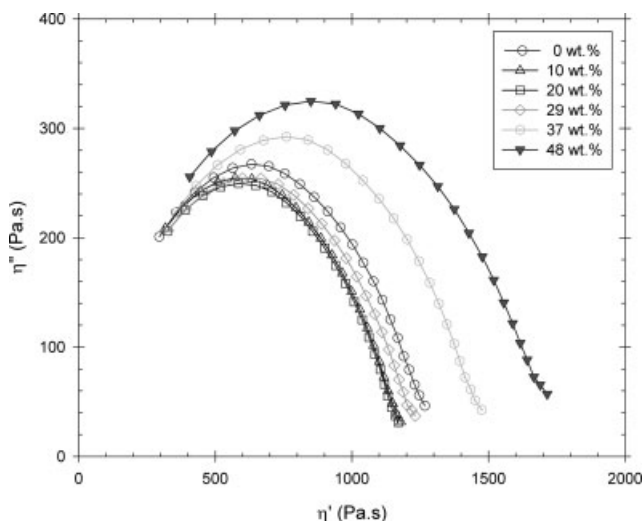
Figure 5 The Cole–Cole plots for various filled PEBA compounds at different loading concentrations of BaSO$_4$.

Figure 6 Uniaxial tensile curves for various filled PEBA compounds at different loading concentrations of BaSO$_4$.

It has been reported that the Cole–Cole plot of real part (η') versus imaginary part (η'') of complex viscosity (η^*) may be arguably used to measure the miscibility (or extent of mixing) in a multicomponent polymer system like polymer blend and filled polymers.[27,28,35] A smooth, semicircular shaped curve of the plot could qualitatively suggest good miscibility of the compound components, that, phase homogeneity in the melt, while any deviation from the semicircular shape may indicate the occurrence of nonhomogeneous dispersion and phase segregation due to immiscibility of the components. It is generally recognized[27,28,35] that due to the existence of "yield" stresses in structured fluid states, typical filled polymer systems display the inflection from semicircular shape when the filler loadings are higher than a certain critical value. Figure 5 gives the Cole–Cole plot for pure PEBA resin and various BaSO$_4$-filled compounds at 200°C. It can be observed that all the curves in the plot are smooth and semicircular shaped, implying that the inherent absorption ability of PEBA copolymer onto BaSO$_4$ particles gives rise to good miscibility and dispersion, irrespective of BaSO$_4$ concentrations. For the sake of mixing quality, the above rheological appraisals may deplete the necessity of using various surface treatment methods for improving the dispersion of BaSO$_4$ particles into the PEBA matrix.

Uniaxial tensile properties

In Figure 6, uniaxial tensile test results for various filled PEBA compounds are shown in terms of engineering stress (σ) versus Cauchy (or engineering) strain (ε). Mechanical property parameters, including Young's modulus (E), yield strength and strain (σ_y
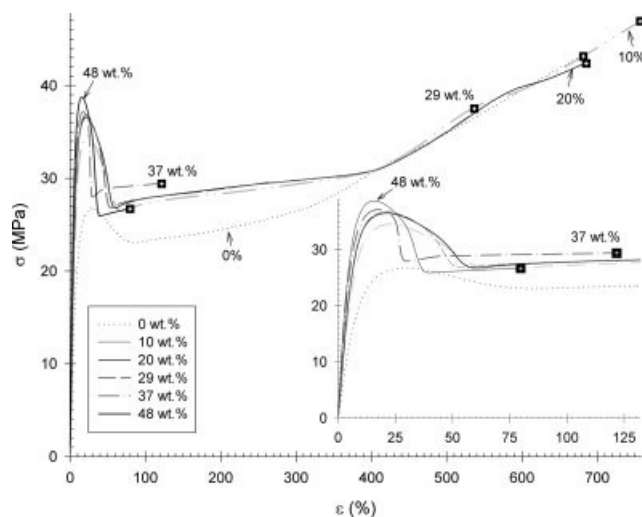
and ε_y), and fracture stress and strain (σ_f and ε_f), are identified and listed in Table I. It is seen that Young's modulus and yield strength of the PEBA compound increases as BaSO$_4$-loading concentration increases. Evidently, BaSO$_4$ particles have strong reinforcement effects on some mechanical properties of the PEBA copolymer by improving material stiffness and yield strength. These effects may be not only related to apparent nucleating effects of BaSO$_4$ for the PEBA copolymer,[2–5,36,37] but also to the polymer absorption by the rigid, inorganic BaSO$_4$ particles as discussed earlier.[30,31,38]

As implied by the above rheology measurements, inherent compatibility between BaSO$_4$ and PEBA copolymer tends to expand the polymer free volume due to polymer interfacial absorption onto the particles. This will help maintaining or even improving material ductility and postyield strain hardening for the filled compounds at low BaSO$_4$ concentrations less than 29 wt %. However, this trend is also counter balanced by the increasing formation of particle aggregates due to the increasing filler–filler interaction when the BaSO$_4$ concentration is increased. From Figure 6 and Table I, it is clearly shown that

TABLE I
Uniaxial Tensile Properties of PEBA Compounds Filled with Different Loading Concentrations of BaSO$_4$

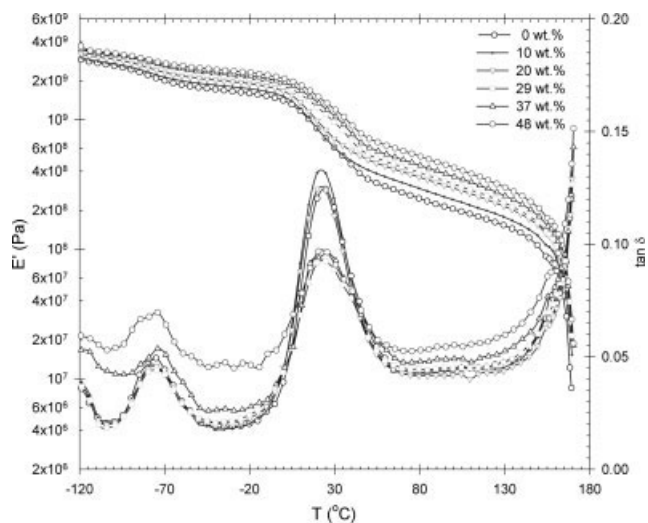| BaSO$_4$ (% w/w)	E (MPa)	σ_y (MPa)	ε_y (%)	σ_f (MPa)	ε_f (%)
0	278.2	26.8	29.4	43.5	681.4
10	432.4	34.6	23.5	46.9	757.2
20	481.1	36.5	22.3	42.0	685.3
29	513.9	36.8	22.2	37.5	536.8
37	662.0	37.1	17.8	29.4	124.4
48	740.9	38.8	15.1	26.7	79.5

Figure 7 Dynamic properties versus temperature for various filled compounds at different loading concentrations of BaSO$_4$.

fracture stresses and strains for the compounds with low BaSO$_4$ concentrations (say 10 and 20 wt %) are comparable or even higher than those of the unfilled PEBA copolymer. For the compounds with the loadings higher than 29 wt %, the postyield strain-hardening behavior completely disappears along with drastic reduction in fracture strain at the expense of overall material ductility and fracture toughness, although the material strengths in terms of yield stresses are still high. The above mechanical behaviors measured under uniaxial tensile tests seemingly correlate with the results of melt rheology as discussed in the preceding section very well.

Dynamic mechanical thermal properties

To explore molecular mechanisms for the peculiarities of mechanical properties as observed in the above uniaxial tensile tests, DMTA test was conducted using the isochronal temperature step scan, and the results are presented in Figure 7. It is readily recognized that storage modulus (E') increases over the whole temperature range as BaSO$_4$ concentration increases, and this is equivalently in line with the change of Young's modulus (E) observed in the uniaxial tensile test, for both Young's modulus and storage modulus are the measurements of material elasticity. With regards to the molecular relaxation mechanisms, both pure PEBA resin and the filled compounds exhibit two glass transitions as revealed by the curves of loss tangent as functions of temperature in Figure 7. In addition, there exists a terminal transition region that is spanned beyond the measurable temperature range higher than 170°C. The lower

glass transition (T_{gf}) can be mainly associated with segmental motion of flexible, amorphous PTMO segments (or amorphous PTMO microdomain) of the PEBA copolymer. The higher glass transition (T_{gr}) can be primarily attributed to the molecular relaxation of amorphous factions in the rigid, crystallizable polyamide segments.[6,10] If the peak temperatures of the loss tangent curves are taken as the glass transitions, the low and high glass transition temperatures can be identified from the curves and are listed in Table II. Apparently, depending of certain BaSO$_4$ loading concentration, the incorporation of BaSO$_4$ filler affects both glass transitions to different extents. From Figure 7 and Table II, what stands out is the fact that for low BaSO$_4$ concentration at 10 wt %, the filled PEBA compound has the sharpest loss tangent at the T_{gr} transition, and both the T_{gf} and T_{gr} glass transitions are reduced to the lowest when compared with these of pure resin and other filled compounds. These facts imply that the PEBA compound filled with 10 wt % BaSO$_4$ has the highest damping ability resultant from the filler-expanded free volume, thus utmostly enhancing the postyield material extensibility and ductility of the PEBA copolymer,[39–41] as observed in Uniaxial tensile properties section. For other PEBA compounds with low BaSO$_4$ concentrations, say 20 and 29 wt %, the similar observations can be marginally made, except that the T_{gr} glass transition (at ca. 22°C) becomes wider with the relevant loss tangent peaks depressed at the transition. The latter is especially true for the compound filled with 29 wt % BaSO$_4$. It is recalled that only the filled compounds with 10, 20, and 29 wt % exhibit the postyield strain-hardening behaviors. Interestingly, these three filled compounds all have the lower T_{gr} and T_{gf} glass transitions than pure resin. As regards the sharpness of loss tangent peaks, it seems that at the BaSO$_4$ concentrations lower than 29 wt %, the filler preferably affect the T_{gr} transition that is only associated to amorphous fractions of PA segments of the copolymer. Therefore, we may assume that the BaSO$_4$ particles may be preferably absorbed onto the PA segments at low concentrations less than 29 wt % BaSO$_4$, reducing chain entanglement and expanding the free volume of the copolymer as a whole. As

TABLE II
Glass Transition Temperatures Measured for Various Filled PEBA Compounds at Different Loading Concentrations of BaSO$_4$

	Weight fractions of BaSO$_4$ (wt.%) of PEBA compounds					
	0	10	20	29	37	48
T_{gf} (°C)	−75.0	−79.0	−76.5	−76.0	−73.5	−73.5
T_{gr} (°C)	24.0	22.0	22.0	22.5	24.0	24.0

$BaSO_4$ concentration further increases in the PEBA compound, the T_{gf} transition starts to increase, becomes wider, and moves toward higher temperature. And simultaneously, the T_{gr} transition continues to be affected, evident by flatter peaks of loss tangent at almost the same peak temperature when compared with pure resin. This may be explained by the fact that the particle aggregates is gradually forming due to strong filler–filler interaction or closer interparticle distances as the $BaSO_4$ concentration increases. These aggregates act as steric hindrance of chain mobility for the entire molecular chains of the copolymer,[30] greatly reducing the damping ability of the copolymer. The formation of particle aggregates of the filler is responsible for the disappearance of the postyield strain-hardening behaviors in the compounds, in which the $BaSO_4$ concentration is higher than a critical value (say 29 wt %). The above DMTA observations agree, quite well, with not only the dynamic viscosity results, but also the uniaxial tensile tests. They can clearly reveal the molecular origins for the measured mechanical and rheological properties of various PEBA compounds filled with different concentrations of barium sulfate particles.

CONCLUSIONS

According to this study, it has been found that $BaSO_4$ filler has apparent reinforcing effects on some mechanical properties of the PEBA copolymer. Young's modulus and yield strength monotonically increases as the loading concentration of $BaSO_4$ increases due to the nucleating effects of $BaSO_4$ and the surface affinity onto the copolymer chains. All the radiopaque compounds studied exhibit the material yielding phenomena before their ultimate tensile fracture. However, the postyield behaviors are strongly dependent on the concentration of $BaSO_4$ loading. At low concentrations near or below 29 wt %, the compounds show the behaviors of strain hardening. As a result, the ultimate fracture stresses are higher than their respective yield strengths, with the ultimate fracture strains being larger than, or comparable to, that of the unfilled PEBA resin. The above effects, as revealed by dynamic rheometry, DSC and DMTA studies, are primarily due to combined effects of accelerated nucleation and crystallization as well as polymer–filler surface affinity and absorption, which are overwhelmingly predominant over the particle–particle interaction-induced steric hindrance to polymer chain mobility. More interestingly, the expansion of the polymer-free volume by the well-dispersed filler particle at low-loading concentration at 10 wt % may toughen the polymer matrix by improving the extensibility of tensile frac-

ture during the postyield strain hardening. However, at high concentrations 37 and 48 wt %, the filler–filler interactions become prominent and would form strong steric hindrance for the chain mobility of the host polymer. Thus, the radiopaque compounds could not exhibit any strain-hardening effects. Consequently, the ultimate fracture stresses and strains are drastically reduced and fall below those of the unfilled PEBA resin. Based on the results of this study, it can be concluded that the synergic balance between mechanical performance and radiopacity for $BaSO_4$-filled radiopaque, biomedical PEBA compounds may be best attained at the loadings around 29 wt % and below.

References

1. Gallardo, V.; Zurita, L.; Ontiveros, A.; Durán, J. D. G. J Pharm Sci 2000, 89, 1134.
2. Hammer, C. O.; Maurer, F. H. J. Polym Compos 1998, 19, 116.
3. Hammer, C. O.; Maurer, F. H. J. Polym Eng Sci 1998, 38, 1295.
4. Ren, Z.; Shanks, R. A.; Rook, T. J. J Appl Polym Sci 2001, 79, 1940.
5. Wang, K.; Wu, J.; Zeng, H. Polym Int 2004, 53, 838.
6. Fakirov, S., Ed.; Handbook of Condensation Thermoplastic Elastomers; Wiley-VCH: Weinheim, Germany, 2005.
7. Legge, N. R.; Holden, G.; Schroeder, H. E. Thermoplastic Elastomers, A Comprehensive Review; Hanser: Munich, 1987.
8. McCrum, N. G.; Read, B. E.; Williams, G. Anelastic and Dielectric Effects in Polymeric Solids; Dover Publications: New York, 1967.
9. Li, L. B.; Koch, M. H. J.; de Jeu, W. H. Macromolecules 2003, 36, 1626.
10. Sheth, J. P.; Xu, J.; Wilkes, G. L. Polymer 2003, 44, 743.
11. Sauer, B. B.; Mclean, R. S.; Londono, D. J. Polym Mater Sci Eng 2001, 85, 268.
12. Sauer, B. B.; Mclean, R. S.; Thomas, R. R. Polym Int 2000, 49, 449.
13. Mclean, R. S.; Sauer, B. B. J Polym Sci Polym. Phys Ed 1999, 37, 859.
14. Hatfield, G. R.; Guo, Y. H.; Killinger, W. E.; Andrejak, R. A.; Roubicek, P. M. Macromolecules 1993, 26, 6350.
15. Veenstra, H.; Hoogvilet, R. M.; Norder, B.; De Boer, A. P. J Polym Sci Part B: Polym Phys 1998, 36, 1795.
16. Han, C. D.; Baek, D. M.; Kim, J. K.; Ogawa, T.; Sakamoto, N.; Hashimoto, T. Macromolecules 1995, 28, 5043.
17. Han, C. D. Macromol 1989, 22, 383.
18. Guo, X. P. Soc Plast Eng ANTEC Tech Pap, 2004, 4244.
19. Yang, I. K.; Tsai, P. H. J Polym Sci Part B: Polym Phys 2005, 43, 2557.
20. Guo. X. P. Soc Plast Engr ANTEC Tech Pap 2007, 968.
21. Leung, L. M.; Koberstein, J. T. Macromolecules 1986, 19, 706.
22. Saiani, A.; Daunch, W. A.; Verbeke, H.; Leenslag, J. W.; Higgins, J. S. Macromolecules 2001, 34, 9059.
23. Kyotani, M. J Polym Sci Part B: Polym Phys 1982, 20, 345.
24. Ramesh, C. Macromolecules 1999, 32, 5704.
25. Rhee, S.; White, J. L. J Polym Sci Part B: Polym Phys 2002, 40, 1189.
26. Hatfield, G. R.; Bush, R. W.; Killinger, W. E.; Roubicek, P. M. Polymer 1994, 35, 3943.
27. Kwag, H.; Rana, D.; Choe, K.; Rhee, J.; Woo, T.; Lee, B. H.; Choe, S. Polym Eng Sci 2000, 40, 1672.
28. Utracki, L. A. In Rheology of Polymer Alloys and Blends, Hanser: Munich, 1989.

29. Macosko, C. W. Rheology: Principles, Measurement, and Applications, Wiley-VCH: New York, 1994.
30. Shenoy, A. V. Rheology of Filled Polymer Systems, Kluwer: New York, 1999.
31. Yanovsky, Y. G. Polymer Rheology: Theory and Practice, Chapman & Hall: New York, 1993.
32. Carreau, P. J.; De Kee, D. C. R.; Chhabra, R. P. Rheology of Polymeric Systems: Principles and Applications, Hanser: New York, 1997.
33. Otsubo, Y. J Colloid and Interface Sci 1986, 112, 380.
34. Doolittle, A. K. J Appl Phys 1951, 22, 1031.
35. Joshi, M.; Butola, B. S.; Simon, G.; Kukaleva, N. Macromolecules 2006, 39 1939.
36. Yuksekkalayci, C.; Yilmazer, U.; Orbey, N. Polym Eng Sci 1999, 39, 1216.
37. Leong, Y. W.; Mohd. Ishak, Z. A.; Ariffin, A. J Appl Polym Sci 2004, 91, 3327.
38. Marcos, A.; de Benito, J. L.; Ibarra, L.; Rodriguez, A.; González, L. Polym Int 1991, 25, 7.
39. Galperin, I.; Carter, J. H.; Hein, P. R. J Appl Polym Sci 1968, 12, 1751.
40. Botev, M.; Betchev, H.; Bikiaris, D.; Panayiotou, C. J Appl Polym Sci 1999, 74 523.
41. Ward, I. M. Mechanical Properties of Solid Polymers, 2nd ed.; Wiley: New York, 1983.